THE GEOLOGICAL SOCIETY OF AMERICA®

Persistence of a freshwater surface ocean after a snowball Earth

Jun Yang[1], Malte F. Jansen[2], Francis A. Macdonald[3], and Dorian S. Abbot[2]
[1]Department of Atmospheric and Oceanic Sciences, School of Physics, Peking University, Beijing 100871, China
[2]Department of the Geophysical Sciences, University of Chicago, Chicago, Illinois 60637, USA
[3]Department of Earth and Planetary Science, Harvard University, Cambridge, Massachusetts 02138, USA

ABSTRACT

Geochemical data from cap carbonates deposited above Cryogenian glacial deposits have been widely used to infer the conditions that prevailed in the aftermath of snowball Earth. However, the time scale over which these carbonates were deposited and the degree to which they record the chemistry of a globally well-mixed ocean have remained poorly constrained. During deglaciation, a large volume of meltwater entered the ocean, creating two distinct layers: the fresh, hot, and light upper layer, and the salty, cold, and dense lower layer. Here we estimate the ocean mixing time scale based on energetic constraints. We find that the mixing time scale is 10^4–10^5 yr, with a best estimate of ~5×10^4 yr, or up to 100 times longer than that of the modern ocean. Mixing of the surface temperature anomaly implies a delayed sea-level rise of 40–50 m associated with pure thermal expansion. This result reconciles geological, geochemical, and paleomagnetic data from basal Ediacaran cap carbonates with physical oceanographic theory. In particular, our model suggests that (1) the cap dolostones formed predominantly in a freshwater environment; (2) the waters in which the dolostones formed were not well mixed with saline deep water, allowing for large geochemical differences between the cap dolostones and the deep ocean; and (3) the cap carbonate sequences formed in a two-phase transgression that lasted >10^4 yr, which is consistent with both local sea-level records and the preservation of magnetic excursions and reversals.

INTRODUCTION

Geological, paleomagnetic, and geochronological constraints suggest that two low-latitude and long-lived glaciations occurred during the Cryogenian Period and that the terminations of the Sturtian glaciation ca. 660 Ma and the Marinoan glaciation ca. 635 Ma were globally synchronous (Rooney et al., 2015). According to the snowball Earth hypothesis (Kirschvink, 1992; Hoffman and Schrag, 2002), the global mean surface temperature was as low as –50 °C during glaciation, ice sheets existed on continents at all latitudes, and possibly all oceans were overlain by thick sea glaciers. Many inferences about the nature of the glaciations and their aftermath have centered around geochemical, sedimentological, and paleomagnetic data from carbonate rocks that cap the glacial deposits (e.g., Hoffman and Schrag, 2002). These interpretations, however, have been limited by uncertainties in the amount of time recorded in the postglacial transgression and cap carbonate deposition, and in the mixing time scale of the post-snowball Earth ocean. For example, the time scale for deposition of basal Ediacaran cap dolostones, which represents only the lower portion of the entire cap carbonate and postglacial transgressive sequence, has been estimated to vary from >10^3 yr (based on the modern ocean mixing rate; Shields, 2005; Zhang et al., 2001), 10^4 yr (geochemical modeling; Liu et al., 2014), and 10^5 yr (paleomagnetic reversal frequencies, geochemical modeling, and sediment thicknesses; e.g., Font et al., 2010; Kasemann et al., 2014).

In the snowball state, the thickness of continental ice sheets is estimated as 0.7–1.4 km (Liu and Peltier, 2010; but see Benn et al., 2015) and that of sea glaciers as ~1 km (Tziperman et al., 2012), and thus the ocean would have had a salinity of about twice of its present-day value with a temperature close to the freezing point (Ashkenazy et al., 2013; Jansen, 2016). Immediately before deglaciation, the thickness of continental ice sheets may have decreased from its maximum at low CO_2 (Benn et al., 2015), but both the decrease and the CO_2 level required to trigger the deglaciation are highly uncertain. Moreover, the scale of postglacial transgression after the Marinoan glaciation in Namibia is consistent with kilometer-scale continental ice sheets (Hoffman, 2011). Similarly, the depth of sea glaciers at the time of deglaciation would have been somewhat smaller, but still hundreds of meters thick (Abbot et al., 2013). This is because even when surface temperatures in the deep tropics are close to the freezing point, at high latitudes they are still much lower than 0 °C (Fig. 1A). Termination of the snowball Earth is triggered by the continuous accumulation of volcanic CO_2 in the atmosphere over millions of years (Le Hir et al., 2008). As CO_2 concentration reaches a critical threshold, tropical ice begins to melt and all ice melts quickly. The time scale of the melting of ice sheets during the Last Glacial Maximum was <10^4 yr (Peltier, 2004); for snowball Earth, the time scale should be shorter due to the much stronger greenhouse forcing, the lower latitude of ice sheets, and the strong ice albedo feedback. For example, a net surface heating rate of only 10 W m^{-2} can melt a 1-km-thick ice sheet in ~10^3 yr.

After the ice melting, the entire ocean will be covered by a 1–2-km-thick layer of fresh and hot water, with sea surface temperatures as high as 50 °C (Fig. 1A). Thus, the ocean will exhibit two distinct layers, the upper layer being fresh, hot, and light, and the lower layer being salty, cold, and dense (Figs. 1B and 1C). Here we develop a one-dimensional (1-D) vertical (or more precisely diapycnal) mixing model based on energetic constraints to estimate the persistence time scale of the freshwater ocean.

ENERGY SOURCE OF VERTICAL MIXING

In the modern ocean, cold heavy water flows downward to the deep ocean in local regions, such as the Labrador and Weddell Seas and the Denmark Strait; this is balanced by upwelling over much of the rest of the ocean. Due to the stable stratification (i.e., an increasing density with depth) of the ocean, this uplift of the deep seawater requires an increase of gravitational potential energy, which is obtained from the conversion of kinetic energy. The power of the kinetic energy in the deep ocean, related to internal waves and small-scale turbulence, derives mainly from lunisolar tides and surface wind stresses (Wunsch and Ferrari, 2004). Recent work (Waterhouse et al., 2014) shows that tides contribute ~1.5 TW (TW = 10^{12} W) globally, and that winds provide ~0.3 TW for near-inertial wave-driven mixing and ~0.2 TW for lee wave-driven mixing. Most of the ~2 TW turbulent kinetic energy (ε) is dissipated to heat by viscous friction, but a small fraction (Γ), estimated as ~20%, is fed back to the ocean circulation and used to vertically mix the ocean water. The input rate of energy for vertical mixing below the mixed layer is thus $\Gamma \times \varepsilon \cong 0.4$ TW for the modern ocean.

To investigate ocean mixing in the aftermath of a snowball Earth, we need to understand potential changes in the energy sources for mixing. We estimate that the energy input to post–snowball vertical mixing is somewhat

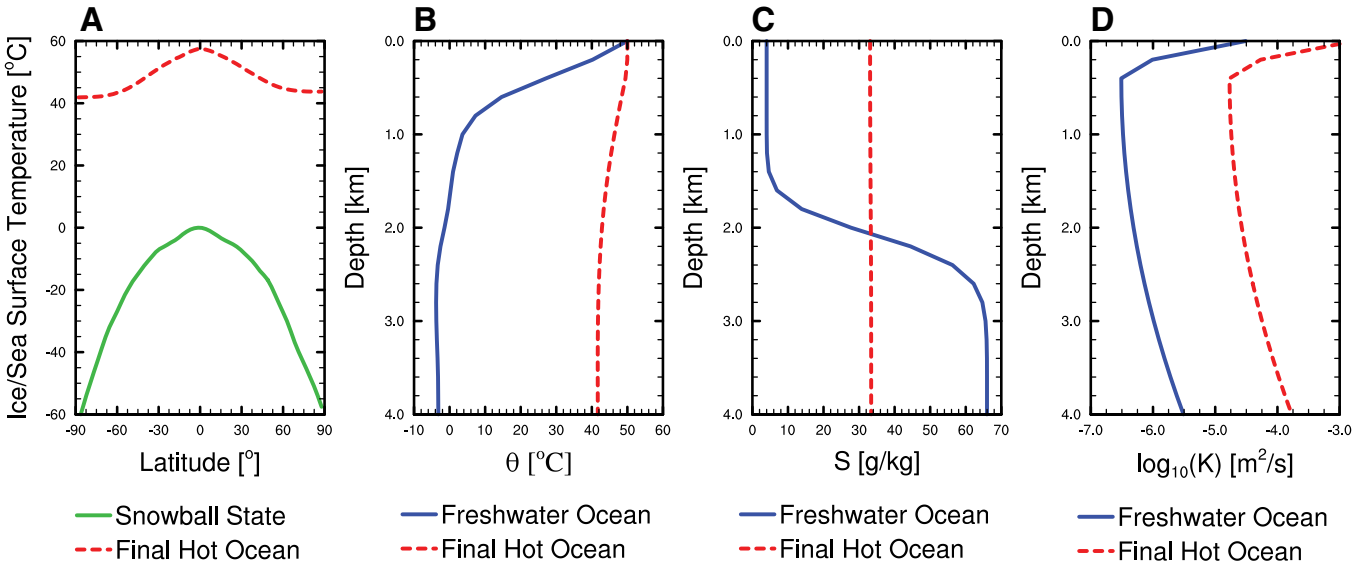

Figure 1. A: Zonal and annual mean sea-surface temperature right before the snowball Earth melting (green) and after the melting (red), simulated by the atmospheric circulation model CAM3 (Collins et al., 2004); solar insolation is 1286 W m^{-2} and CO_2 concentration is 10^5 ppmv. B: Ocean salinity as a function of depth, at the time right after all of the freshwater has entered the ocean (blue) and at the time when the ocean temperature has reached equilibrium (red) in the control run. The two time points, 10^3 and 5.8×10^4 yr, correspond to the vertical solid and dashed lines in Figure 2. C: Same as B, but for potential temperature. D: Same as B, for diapycnal mixing coefficient.

lower than the modern value, ~0.3 TW, because both lunar tides and surface wind stresses in the Cryogenian Period were probably weaker than at present (see the GSA Data Repository[1]). However, the uncertainty range for the energy input to mixing is large, and here taken to be between 0.04 and 1.1 TW (see the Data Repository).

Using an effective turbulent diffusivity to represent the effect of small-scale turbulent motion (Wunsch and Ferrari, 2004), the balance between energy supplied by turbulent dissipation and energy required for vertical mixing becomes

$$\left\langle \kappa N^2 \right\rangle = \Gamma \varepsilon / M_{ocn}, \quad (1)$$

where N^2 is buoyancy frequency, which is a measure of stratification, κ is vertical turbulent diffusivity, and M_{ocn} is the mass of the ocean; the angle brackets denote an average over the entire ocean. For the strongly stratified post-snowball ocean, N^2 is much larger than that in the modern ocean. Given a similar energy input, we would therefore expect the diffusivity κ to be much smaller.

METHOD I. GRAVITATIONAL POTENTIAL ENERGY BUDGET

A rough estimate of the mixing time scale can be made using the conversion of vertical mixing energy ($\Gamma \times \varepsilon$) to gravitational potential energy (GPE). As the initial state, we assume a 2 km, warm, freshwater layer (salinity S_1 = 4 g kg^{-1}, temperature T_1 = 15 °C, height H_1 = 2 km, and potential density ρ_1) overlying a 2 km, cold, salty water layer (S_2 = 66 g kg^{-1}, T_2 = –4 °C, H_2 = 2 km, and ρ_1), as shown in Figure 1. During the evolution, the temperature, salinity, potential density, and height of the ocean change. In the final equilibrium state, the ocean is assumed to be well mixed ($S_1' = S_2'$, $T_1' = 50$ °C, $T_2' = 42$ °C, ρ_1', ρ_2', H_1', and H_2'; the prime denotes the corresponding value after the mixing). The change in potential density follows the equation of state, and changes in salinity and height follow conservation of mass. The change of GPE is

$$\Delta GPE = \left[\frac{1}{2} \rho_2' g H_2' + \rho_1' g H_1' \left(H_2' + H_1'/2 \right) \right] - \left[\frac{1}{2} \rho_2 g H_2^2 + \rho_1 g H_1 \left(H_2 + H_1/2 \right) \right]. \quad (2)$$

The mixing time scale is $t = (\Delta GPE \times A_{ocn})/(\Gamma \times \varepsilon)$, where A_{ocn} is the ocean area (3.6×10^{14} m^2), ($\Gamma \times \varepsilon$) is 0.3 TW, and ΔGPE is 1.9×10^9 J m^{-2}. Thus, t is 7.2×10^4 yr. During the entire process, the increase of ocean depth ($H_1' + H_2' - H_1 - H_2$) is 48 m, which is the value of sea-level rise due to the pure thermal expansion of seawater. Note that this calculation uses potential density rather than in situ density, meaning that we have ignored the pressure dependency. This simplification is adequate for our purposes because the contribution of the pressure correction on density before and after mixing approximately cancels.

METHOD II. 1D VERTICAL MIXING MODEL

We simulate the evolution of the highly stratified post-snowball ocean using a one-dimensional (1-D) vertical diffusion equation:

$$\frac{\partial C}{\partial t} - \frac{\partial}{\partial z}\left(\kappa \frac{\partial C}{\partial z} \right) = 0, \quad (3)$$

where C is salinity or potential temperature. The boundary conditions at the top and bottom boundaries are no flux for salinity, fixed temperature at the upper boundary, and fixed geothermal heat flux at the bottom boundary. Details of the numerical model are provided in the Data Repository; the key feature is the time-dependent vertical κ, the magnitude of which is computed following the energy budget in Equation 1, with a prescribed rate of energy input $\Gamma \times \varepsilon$ = 0.3 TW by default. The freshwater is assumed to enter the ocean in a time scale of 10^3 yr, and sensitivity tests (10^2 and 10^4 yr; Table 1) show that this does not influence the conclusion.

The results of the model are shown in Figure 2. The time scale of ocean mixing in the control run is ~5.2×10^4 yr, and the sea-level rise due to pure thermal expansion is 45 m. Comparing Figures 2A and 2B indicates that the time required for the mixing of salinity is ~10% shorter than that for temperature. This is due to the differences in the initial and boundary conditions for temperature and salinity. After the addition of the freshwater layer, the salinity profile has a sharp gradient at mid-depth, while high temperatures are confined closer to the sea surface where they are imposed as a boundary condition.

Figure 2 indicates that during the evolution phase, vertical mixing has the effect of transporting salt from the deep ocean to the upper ocean and transporting heat from the sea surface into the deep ocean. The net effect of these transports is a reduction in the density difference between

[1]GSA Data Repository item 2017201, methods and Figures DR1 and DR2, is available online at http://www.geosociety.org/datarepository/2017/ or on request from editing@geosociety.org.

TABLE 1. TIME SCALE FOR COMPLETING OCEAN MIXING OF SALINITY AND TEMPERATURE AND SEA-LEVEL RISE DUE TO PURE THERMAL EXPANSION AFTER SNOWBALL EARTH DEGLACIATION

Runs	Experimental design	t_{salt} (yr)	t_{temp} (yr)	ΔSL_{TE} (m)
Control	Freshwater depth = 2 km, κ follows Figure 1D and Equation 1, geothermal heat = 0.1 W m^{-2}, sea-surface temperature = 50 °C, mixing energy = 0.3 TW, and freshwater enters the ocean in 10^3 yr	5.2×10^4	5.8×10^4	45
Sensitivity 1	Decrease the mixing energy from 0.3 to 0.04 TW	1.9×10^5	1.4×10^5	41
	Increase the mixing energy from 0.3 to 1.1 TW	1.5×10^4	1.9×10^4	44
Sensitivity 2	Decrease the freshwater depth from 2.0 to 1.6 km	4.7×10^4	5.4×10^4	42
	Decrease the freshwater depth from 2.0 to 1.0 km	3.8×10^4	4.8×10^4	41
Sensitivity 3	Freshwater enters the ocean in 10^2 yr	5.2×10^4	5.8×10^4	44
	Freshwater enters the ocean in 10^4 yr	5.2×10^4	5.9×10^4	36
Sensitivity 4	Fix κ to be a constant of 6×10^{-6} m^2 s^{-1}	4.1×10^4	4.6×10^4	46
	Fix κ to be the modern value of 3×10^{-5} m^2 s^{-1}	7.1×10^3	1.4×10^4	44
Sensitivity 5	Increase geothermal heat from 0.1 to 0.2 W m^{-2}	4.6×10^4	4.6×10^4	45
	Decrease geothermal heat from 0.1 W m^{-2} to zero	6.0×10^4	7.9×10^4	45

Note: TW = 10^{12} W; κ is vertical turbulent diffusivity; t_{salt} is time of complete ocean mixing of salinity; t_{temp} is temperature; SL_{TE} is sea-level rise due to thermal expansion.

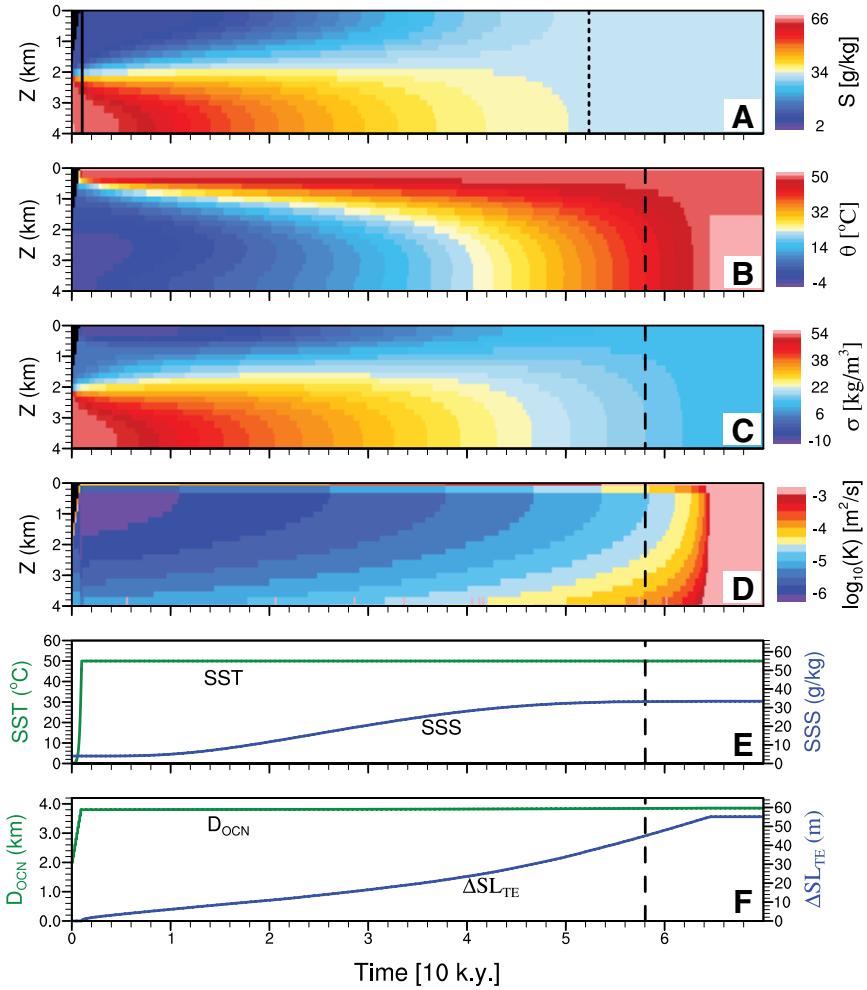

Figure 2. A: Evolution of ocean salinity of a post-snowball Earth in the control run. B: Potential temperature. C: Potential density (1000 kg m^{-3} have been subtracted). D: Diapycnal mixing coefficient. E: Sea-surface temperature (SST, green) and sea-surface salinity (SSS, blue). F: Ocean depth (D_{OCN}, green) and sea-level rise due to pure thermal expansion (ΔSL_{TE}, blue) of a post-snowball Earth in the control run (see text and the Data Repository [see footnote 1] for experimental design). Salinity and temperature complete their mixing in ~5.2×10^4 yr (vertical dotted line) and ~5.8×10^4 yr (vertical dashed line), respectively, at which time salinity becomes nearly uniform in depth and the ocean bottom temperature reaches 42 °C and thus equals the expected SST at the poles (Fig. 1A), respectively. The vertical solid line denotes the time at which all of the freshwater has entered the ocean, 10^3 yr. The SST is fixed to 50 °C after all of the freshwater has entered the ocean (see the Data Repository).

the upper and deep ocean, i.e., a weakening of the vertical stratification (Fig. 2C). As the vertical stratification becomes weaker with time, the diffusion coefficient becomes larger (Fig. 2D). Note that near the bottom of the ocean, a temperature inversion (cold water over warm water; Fig. 2B) develops during the early stage of the integration that arises from geothermal heating.

The mixing energy input has a large uncertainty between 0.04 and 1.1 TW, which causes the largest uncertainty in our estimate of the time scale (Table 1). Sensitivity tests show that for the upper limit of the mixing energy input, the mixing time scale is 1.5×10^4 yr, and for the lower limit, the time scale is 1.9×10^5 yr. The depth of the upper freshwater layer has a range of uncertainty due to uncertainty in ice sheet depth (Liu and Peltier, 2010) and in sea glacier thickness (Abbot et al., 2013). Tests show that decreasing the freshwater layer depth from 2 to 1.6 km leads to a somewhat shorter time scale of 4.7×10^4 yr, and for a freshwater layer depth of 1 km, the time scale is 3.8×10^4 yr. Changing the time period over which the freshwater enters into the ocean has a negligible effect on the mixing time scale. For a given turbulent diffusivity, κ, the time scale is approximately inversely proportional to κ. If κ is set to be a constant of 6×10^{-6} m^2 s^{-1}, the time scale is 4.1×10^4 yr. For a present-day κ of 3×10^{-5} m^2 s^{-1} (although unrealistic for the post-snowball ocean), the time scale would be 7.1×10^3 yr. Geothermal heat flux warms the ocean at the bottom, which results in an additional energy source. Doubling the geothermal heat flux therefore decreases the time scale by 12%, while setting the geothermal heat flux to zero increases the time scale by 15%. Geothermal heat flux becomes more important for extremely weak vertical mixing.

Figure 2 shows that after reaching equilibrium, potential temperature and potential density are uniform in depth, which is unrealistic and is mainly due to the absence of vertical and horizontal advection in the 1-D model. However, the lack of advection becomes important only in the last ~10^4 yr before reaching equilibrium, and thus does not significantly affect the bulk timescale estimates. The 1-D model should become invalid once the deep ocean density becomes smaller than the densest waters near the surface (typically found near the poles), at which point high-latitude convection and deep ocean circulation begin. Inferring high-latitude surface temperatures based on a 3-D atmospheric model simulation shown in Figure 1A, we estimate that high-latitude deep convection will not begin until near the very end of our simulations.

DISCUSSION

The lack of a robust age model has severely limited interpretations of geochemical, sedimentological, and paleomagnetic data from cap carbonates. Our result of 10^4–10^5 yr of mixing

time for the meltwater plume suggests that cap dolostones formed predominantly in a freshwater environment. Geochemical data from cap carbonates should be interpreted in the context of a mixing model with a 10^4–10^5 yr residence time between distinct reservoirs, rather than a well-mixed ocean (cf. Kasemann et al., 2014). This framework is also in line with recent Mg and Sr isotopes studies that argue that the cap carbonate and overlying sediments were deposited in two geochemically distinct fluids (Liu et al., 2014; Hoffman, 1999), and thus the lack of mantle-like Sr isotope values in postglacial sediments cannot be used as an argument against the snowball Earth hypothesis (cf. Kennedy et al., 2001).

The late sea-level rise of 40–50 m due to pure thermal expansion is an important feature to include in post-snowball sea-level models (Creveling and Mitrovica, 2014) and in interpreting geochemical and stratigraphic records of the snowball aftermath. We propose that basal Ediacaran cap dolostones formed during postglacial melting, and that the remaining sea-level rise recorded between the top of the cap dolostone and the maximum flooding surface higher in the cap carbonate sequence corresponds to the thermal expansion of the ocean. Thus, the age model presented here reconciles estimates of cap carbonate deposition inferred from physical oceanography (>10^3 yr using modern ocean mixing rate; Shields, 2005; Zhang et al. 2001) with geological, geochemical, and geophysical data (10^4–10^6 yr from geochemical modeling, paleomagnetic reversal frequencies, and sediment thicknesses; e.g., Font et al., 2010; Liu et al., 2014; Kasemann et al., 2014).

CONCLUSION

Based on energetic constraints, we find that the mixing time scale of a post-snowball ocean is ~10^4 to 10^5 yr, which is up to100 times longer than that of the modern ocean. This result reconciles physical theory with geological constraints and suggests that basal Ediacaran cap dolostones formed predominantly in the freshwater layer of a strongly stratified ocean during a prolonged postglacial transgression. We also show that after all of the freshwater has entered the ocean, the post-snowball sea-level rise due to pure thermal expansion is significant, ~40–50 m, which may explain the extended transgression recorded in basal Ediacaran cap carbonate sequences above the cap dolostone.

ACKNOWLEDGMENTS

We are grateful to Yonggang Liu and Dawei Li for their insightful discussions. We thank Paul F. Hoffman, Galen Halverson, and an anonymous reviewer for their helpful comments and suggestions. Yang is supported by National Science Foundation of China grant 41606060. Model source code and data are available from junyang@pku.edu.cn.

REFERENCES CITED

Abbot, D.S., Voigt, A., Li, D., Le Hir, G., Pierrehumbert, R.T., Branson, M., Pollard, D., and Koll, D.D.B., 2013, Robust elements of Snowball Earth atmospheric circulation and oases for life: Journal of Geophysical Research, v. 118, p. 6017–6027, doi:10.1002/jgrd.50540.

Ashkenazy, Y., Gildor, H., Losch, M., Macdonald, F.A., Schrag, D.P., and Tziperman, E., 2013, Dynamics of a Snowball Earth ocean: Nature, v. 495, p. 90–93, doi:10.1038/nature11894.

Benn, D.I., Le Hir, G., Bao, H., Donnadieu, Y., Dumas, C., Fleming, E.J., Hambrey, M.J., McMillan, E.A., Petronis, M.S., and Ramstein, G., 2015, Orbitally forced ice sheet fluctuations during the Marinoan Snowball Earth glaciation: Nature Geoscience, v. 8, p. 704–707, doi:10.1038/ngeo2502.

Collins, W.D., et al., 2004, Description of the NCAR Community Atmosphere Model CAM3.0: National Center for Atmospheric Research (NCAR) Technical Note NCAR/TN-464 STR, 226 p., http://www.cesm.ucar.edu/models/atm-cam/docs/description/description.pdf (accessed February 2017).

Creveling, J., and Mitrovica, J.X., 2014, The sea-level fingerprint of a Snowball Earth deglaciation: Earth and Planetary Science Letters, v. 399, p. 74–85, doi:10.1016/j.epsl.2014.04.029.

Font, E., Nédélec, A., Trindade, R., and Moreau, C., 2010, Fast or slow melting of the Marinoan snowball Earth? The cap dolostone record: Palaeogeography, Palaeoclimatology, Palaeoecology, v. 295, p. 215–225, doi:10.1016/j.palaeo.2010.05.039.

Hoffman, P.F., 1999, The break-up of Rodinia, birth of Gondwana, true polar wander and the snowball Earth: Journal of African Earth Sciences, v. 28, p. 17–33, doi:10.1016/S0899-5362(99)00018-4.

Hoffman, P.F., 2011, Strange bedfellows: Glacial diamictite and cap carbonate from the Marinoan (635 Ma) glaciation in Namibia: Sedimentology, v. 58, p. 57–119, doi:10.1111/j.1365-3091.2010.01206.x.

Hoffman, P.F., and Schrag, D.P., 2002, The Snowball Earth hypothesis: Testing the limits of global change: Terra Nova, v. 14, p. 129–155, doi:10.1046/j.1365-3121.2002.00408.x.

Jansen, M.F., 2016, The turbulent circulation of a snowball Earth Ocean: Journal of Physical Oceanography, v. 46, p. 1917–1933, doi:10.1175/JPO-D-15-0224.1.

Kasemann, S.A., von Strandmann, P.A.P., Prave, A.R., Fallick, A.E., Elliott, T., and Hoffmann, K.-H., 2014, Continental weathering following a Cryogenian glaciation: Evidence from calcium and magnesium isotopes: Earth and Planetary Science Letters, v. 396, p. 66–77, doi:10.1016/j.epsl.2014.03.048.

Kennedy, M.J., Christie-Blick, N., and Prave, A.R., 2001, Carbon isotopic composition of Neoproterozoic glacial carbonates as a test of paleoceanographic models for snowball Earth phenomena: Geology, v. 29, p. 1135–1138, doi:10.1130/0091-7613(2001)029<1135:CICONG>2.0.CO;2.

Kirschvink, J.L., 1992, Late Proterozoic low-latitude global glaciation: The Snowball Earth, *in* Schopf, J.W., and Klein, C., eds., The Proterozoic biosphere: Cambridge, UK, Cambridge University Press, p. 51–52.

Le Hir, G., Ramstein, G., Donnadieu, Y., and Goddéris, Y., 2008, Scenario for the evolution of atmospheric pCO_2 during a snowball Earth: Geology, v. 36, p. 47–50, doi:10.1130/G24124A.1.

Liu, C., Wang, Z., Raub, T.D., Macdonald, F.A., and Evans, D.A., 2014, Neoproterozoic cap-dolostone deposition in stratified glacial meltwater plume: Earth and Planetary Science Letters, v. 404, p. 22–32, doi:10.1016/j.epsl.2014.06.039.

Liu, Y., and Peltier, W.R., 2010, A coupled carbon cycle-climate model of Neoproterozoic glaciation: Influence of continental configuration on the formation of a "Soft Snowball": Journal of Geophysical Research, v. 115, D17111, doi:10.1029/2009JD013082.

Peltier, W.R., 2004, Global glacial isostasy and the surface of the ice-age Earth: The Ice-5G (VM2) Model and GRACE: Annual Reviews of Earth and Planetary Science, v. 32, p. 111–149, doi:10.1146/annurev.earth.32.082503.144359.

Rooney, A.D., Strauss, J.V., Brandon, A.D., and Macdonald, F.A., 2015, A Cryogenian chronology: Two long-lasting, synchronous Neoproterozoic glaciations: Geology, v. 43, p. 459–462, doi:10.1130/G36511.1.

Shields, G.A., 2005, Neoproterozoic cap carbonates: A critical appraisal of existing models and the plume world hypothesis: Terra Nova, v. 17, p. 299–310, doi:10.1111/j.1365-3121.2005.00638.x.

Tziperman, E., Abbot, D.S., Ashkenazy, Y., Gildor, H., Pollard, D., Schoof, C., and Schrag, D.P., 2012, Continental constriction and sea ice thickness in a snowball-Earth scenario: Journal of Geophysical Research, v. 117, C05016, doi:10.1029/2011JC007730.

Waterhouse, A.F., et al., 2014, Global patterns of diapycnal mixing from measurements of the turbulent dissipation rate: Journal of Physical Oceanography, v. 44, p. 1854–1872, doi:10.1175/JPO-D-13-0104.1.

Wunsch, C., and Ferrari, R., 2004, Vertical mixing, energy, and the general circulation of the oceans: Annual Review of Fluid Mechanics, v. 36, p. 281–314, doi:10.1146/annurev.fluid.36.050802.122121.

Zhang, R., Follows, M.J., Grotzinger, J.-P., and Marshall, J., 2001, Could the Late Permian deep ocean have been anoxic?: Paleoceanography, v. 16, p. 317–329, doi:10.1029/2000PA000522.

Manuscript received 27 December 2016
Revised manuscript received 2 March 2017
Manuscript accepted 17 March 2017

Printed in USA

Supplemental Material for "Persistence of a freshwater surface ocean after a snowball Earth"

Jun Yang, Malte F. Jansen, Francis A. Macdonald, and Dorian S. Abbot

METHODS

Estimating the Energy Input to Deep Ocean Mixing

To understand post-snowball mixing, we need to understand potential changes in the energy sources for vertical mixing. The largest energy source to deep ocean mixing arises from tidal flows (e.g., Waterhouse et al., 2014). Based on the analysis of sedimentary cyclic rhythmites of tidal origin, Williams (2000) suggested that the average rate of energy dissipation by the lunar tide since the cryogenic period was about 40% smaller than today[1]. **The present rate of tidal energy dissipation thus appears to be unusually large, likely due to resonances associated with the specific continental configuration (Green et a., 2017)**. **The moon was closer than today, but only by a few percent (<5%), which has a comparatively small effect.** As tidal energy dissipation has likely varied non-monotonically during the last 700 million years (e.g., due to changes in the continental configuration), the rate of tidal energy dissipation during the ice-free periods of the cryogenic itself is less well constraint, but much larger dissipation rates than today appear to be unlikely. Less than 50% of the total tidal energy dissipation is presently transferred into internal waves, which can break and contribute to vertical mixing in the ocean

[1] The average tidal energy dissipation can be inferred from the rate of change in the moon's orbital radius. The orbital radius has **increased** by an average of about 2.2 cm/year since the late Neoproterozoic, which corresponds to just over half the present rate, **3.8 cm/year** (e.g., Williams, 2000). Since total changes in the orbital radius over this time period have been relatively small (<~5%), the energy dissipation rate is approximately linearly proportional to the rate of change of the orbital radius.

interior (Wunsch and Ferrari, 2004). The rest is dissipated on shallow shelves or in the bottom boundary layer. The fraction of tidal energy that is transferred into internal waves depends primarily on the abyssal stratification and bottom topographic roughness (Jayne and St. Laurent, 2001). While the interior ocean would be highly stratified in the aftermath of a snowball Earth event, the abyss would likely lose its stratification relatively quickly (see Fig. 2 in the main text), thus potentially making the conversion of tidal energy much less efficient. Topographic roughness is controlled largely by tectonic processes, and is unlikely to have changed very much. In the following, we assume the tidal power input to interior-ocean turbulence to be 60% of the present-day value of ~1.5 TW (TW: 10^{12} W; Waterhouse et al., 2014), i.e., 0.9 TW, but with a plausible range between 0.3-2.7 TW.

An additional source of energy for mixing arises from wind-driven near-inertial and geostrophic ocean currents. For the present-day, this energy input amounts to about 0.5 TW (Wunsch and Ferrari, 2004; Waterhouse et al., 2014). Due to the very small equator-to-pole surface temperature difference (Fig. 1 in the main text) after the snowball, surface wind stresses over the ocean would likely be smaller than today, as can be seen in simulations using a 3D atmospheric circulation model (Fig. DR1 below). The result suggests a reduction in wind energy input. Assuming that surface current speeds are to first order proportional to the magnitude of the wind stress, the total wind work is expected to scale with the square of the wind stress, which in turn is estimated to be reduced to ~60% of today's value. In the following, we assume a wind-driven power input to interior ocean turbulence of 0.3 TW, with a large uncertainty range of 0.1-0.9 TW. We therefore estimate the total interior turbulent dissipation (ε) as ~1.2 TW, with an uncertainty range between 0.4 and 3.6 TW. Notice that we conservatively added uncertainties for tidal and wind-driven energy dissipation linearly.

The mixing efficiency Γ is generally assumed to be 0.2, based on Osborn (1980). Theoretical and experimental studies show that the value of Γ depends non-monotonically on the local Richardson number (Peltier and Caulfield, 2003), but we have little reason to believe that the average mixing efficiency has changed substantially between the present and post-snowball climates. Moreover, a much larger value than the canonical $\Gamma = 0.2$ can be excluded on theoretical and experimental grounds (Ivey et al., 2008). Here we assume $\Gamma = 0.2$, with an uncertainty range between 0.1 and 0.3. This yields an energy input to vertical mixing of $\Gamma \times \varepsilon = 1.2 \times 0.2 \sim 0.3$ TW, with a conservative uncertainty range between 0.04 and 1.1 TW.

1-D Mixing Model Setup

We integrate the 1D mixing equation (Eq. (3) of the main text) with an initial state of a 2-km deep layer of cold and salty water. In the control run, we add a 2-km freshwater layer at a constant rate of 2 m per year. The potential temperature, salinity, and diffusion coefficient at the time right after all of the freshwater has entered the ocean are shown in Fig. 1 (blue lines) of the main text. We prescribe a fixed vertical structure for the diffusion coefficient, which is enhanced near the surface and at the ocean bottom to account for the effects of surface winds and bottom topography, respectively (Fig. 1D). The magnitude of the eddy diffusivity evolves in time and is computed following Eq. (1) of the main text, with a fixed energy input rate $\Gamma \times \varepsilon$. For very small N^2, the diffusion coefficient will be large enough to induce numerical instability. We avoid this by introducing an upper limit of 0.01 $m^2\ s^{-1}$. This has a very small effect on the result, since N^2 becomes small during the final stage of the simulation. We also include a lower limit of 10^{-7} $m^2\ s^{-1}$, which corresponds to the molecular diffusivity of heat.

When the density profile is unstable with dense water overlying light water, convection will occur, which is parameterized by setting the diffusion coefficient to a large value of 0.01 m^2 s^{-1}, as is done in global ocean circulation models (e.g., Smith et al., 2010). In our calculations, convection mostly occurs near the bottom of the ocean, where the geothermal heat flux acts to destabilize the seawater. The ocean has a depth of 4 km with 21 vertically uniform levels. The time step is 0.025 year. The equation of state of seawater employed here and in METHOD I of the main text is that of Millero and Huang (2009), which is valid for wide ranges of salinity (5 to 70 g kg^{-1}) and potential temperature (0 to 90 ^{o}C).

During the evolution of the post-snowball ocean, the change of vertical diffusivity is not a monotonic function of time, particularly during the phase of freshwater addition (see Fig. 2D of the main text). In the snowball state and at the beginning of the melting, the ocean has nearly uniform salinity (about 66 g kg^{-1}) and uniform temperature (close to the freezing point), thus, vertical stratification is weak and the diffusivity is large, close to the convection limit of 0.01 m^2 s^{-1}. When freshwater is added to the ocean, stratification increases and the diffusivity decreases. At the time when all of the freshwater has been added to the ocean, vertical stratification reaches its maximum and the diffusivity reaches its minimum. After that, the ocean mixing acts to decrease the stratification, so that the diffusivity increases with time, according to Eq (1) in the main text. Sensitivity tests show that the detailed evolutions of diffusivity and sea surface temperature in the phase of freshwater addition have no significant effect on the bulk timescale estimates and have a small effect (<5 m) on the magnitude of sea level rise associated with pure thermal expansion.

In the model, the surface temperature is fixed to 50 ^{o}C after all of the freshwater has entered the ocean. This is based on the result of a 3D global climate model, CAM3. The

model solves the primitive equations of atmospheric motion on a rotating sphere and the equations for realistic radiative transfer and parameterized convection, condensation, precipitation, clouds, and boundary turbulence (Collins et al., 2004; Boville et al., 2006). It is a standard model that climate scientists employ for simulating the climates of Earth in the past, present, and future. Different types of climate models, including energy balance models (Hoffman and Schrag, 2002; Pierrehumbert et al., 2011) and a 3D global climate model (Le Hir et al., 2008), have also been employed to estimate the post-snowball surface temperature. All of these models found that the post-snowball surface temperature is 50 ^{o}C or greater due to the high concentration of atmospheric CO_2 and strong water vapor feedback.

Based on the estimation of a combined climate-weathering model (Le Hir et al., 2008), the timescale of the silicate weathering cycle to decrease the post-snowball CO_2 concentration is 10^6 years, much longer than previously thought (such as Hoffman and Schrag, 2002). Although the surface temperature is high, continental runoff might be only ~1.2 times the modern runoff (Le Hir et al., 2008b). This is due to the fact that precipitation (and hence runoff) is limited by the supply of solar radiation absorbed at the surface, rather than the surface temperature (Pierrehumbert, 2002). The silicate weathering timescale (10^6 years) is about 10 times the maximum ocean mixing timescale estimated here (10^5 years), so that the assumption of fixed surface temperature of 50 ^{o}C in our model is reasonable.

Finally, we note that most present-day 3D ocean models are not suitable for simulating the post-snowball ocean, as spurious, non-physical numerical diffusion in the models (e.g., Griffies

et al., 2000) may be comparable to or even larger than the small diffusivity of the post-snowball ocean. This is the reason we develop a 1D mixing model.

REFERENCES

Boville, B.A., Rasch, P.J., Hack, J.J. & McCaa, J.R., 2006, Representation of clouds and precipitation processes in the Community Atmosphere Model version 3 (CAM3): J. Climate v. 19, p. 2162-2183.

Green, J.A.M., Huber, M., Waltham, D., Buzan, J., and Wells, M., 2017, Explicitly modelled deep-time tidal dissipation and its implication for Lunar history: Earth and Planetary Science Letters, v. 461, p. 46-53.

Griffies, S.M., Pacanowski, R.C., and Hallbergm R.W., 2000, Spurious Diapycnal Mixing Associated with Advection in a z-Coordinate Ocean Model: Monthly Weather Review, v. 128, p. 538-564, doi:10.1175/1520-0493(2000)128<0538:SDMAWA>2.0.CO;2.

Ivey, G.N., Winters, K.B., and Koseff, J.R., 2008, Density stratification, turbulence, but how much mixing? Annual Review of Fluid Mechanics, v. 40, no. 1, p. 169-184.

Jayne, S.R., and St Laurent, L.C., 2001, Parameterizing tidal dissipation over rough topography: Geophysical Research Letters, v. 28, no. 5, p. 811-814.

Le Hir, G., *et al.*, 2008b, The snowball Earth aftermath: Exploring the limits of continental weathering processes: Earth Planet. Sci. Lett., doi:10.1016/j.epsl.2008.11.010.

Millero, F.J., and Huang, F., 2009, The density of seawater as a function of salinity (5 to 70 g kg^{-1}) and temperature (273.15 to 363.15 K): Ocean Science, v. 5, p. 91-100.

Osborn, T.R., 1980, Estimates of the local rate of vertical diffusion from dissipation measurements: Journal of Physical Oceanography, v. 10, no. 1, p. 83-89.

Peltier, W.R., and Caulfield, C.P., 2003, Mixing Efficiency Stratified Shear Flows: Annual Review of Fluid Mechanics, v. 35, p. 135-167.

Pierrehumbert, R.T., 2002, The hydrologic cycle in deep-time climate problems: Nature, v. 419, p. 191–198.

Pierrehumbert, R.T., Abbot, D.S., Voigt, A., and Koll D.B. D., 2011, Climate of the Neoproterozoic: Annual Review of Earth and Planetary Sciences, v. 39, p. 417-460.

Smith, R., et al., 2010, The Parallel Ocean Program (POP) reference manual: Ocean component of the Community Climate System Model (CCSM): Los Alamos National Laboratory Report LAUR-10-01853, 140 p.

Williams, G.E., 2000, Geological constraints on the Precambrian history of Earth's rotation and the Moon's orbit, Rev. Geophys., v. 38, no. 1, p. 37–59.

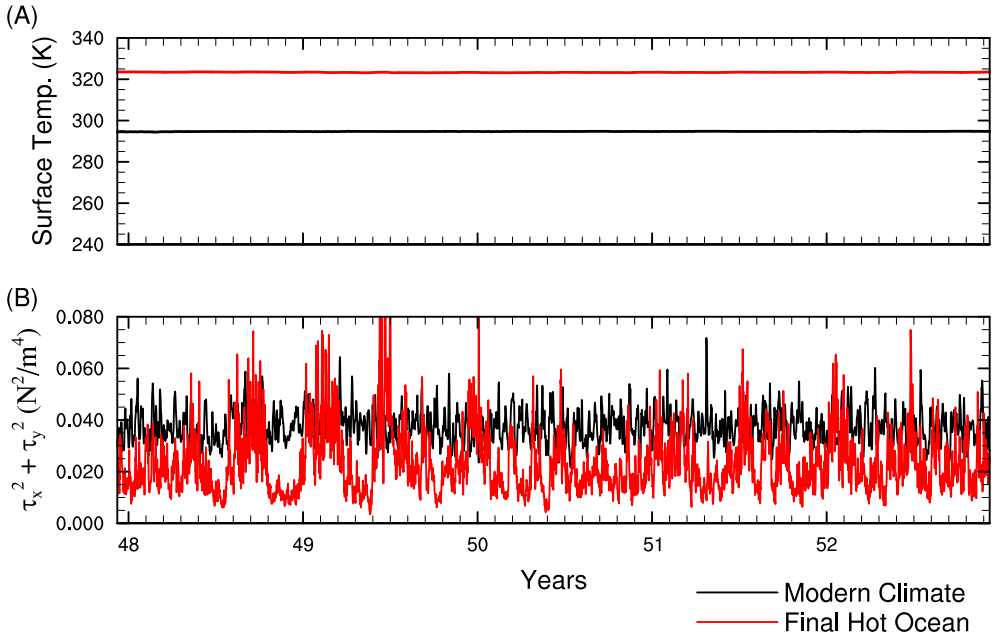

Figure DR1. Time series of global-mean surface temperature (A) and the square of surface wind stresses over oceans (B), simulated by the atmospheric circulation model CAM3. Black line: modern condition, and red line: the final equilibrium post-snowball ocean. The time interval is 12 hours in this plot. For a long-term mean, the global mean of the square of surface wind stresses in the post-snowball condition is about 60% of that in the modern condition, due to the fact that the meridional temperature gradients in the post-snowball condition are relatively weaker.

156

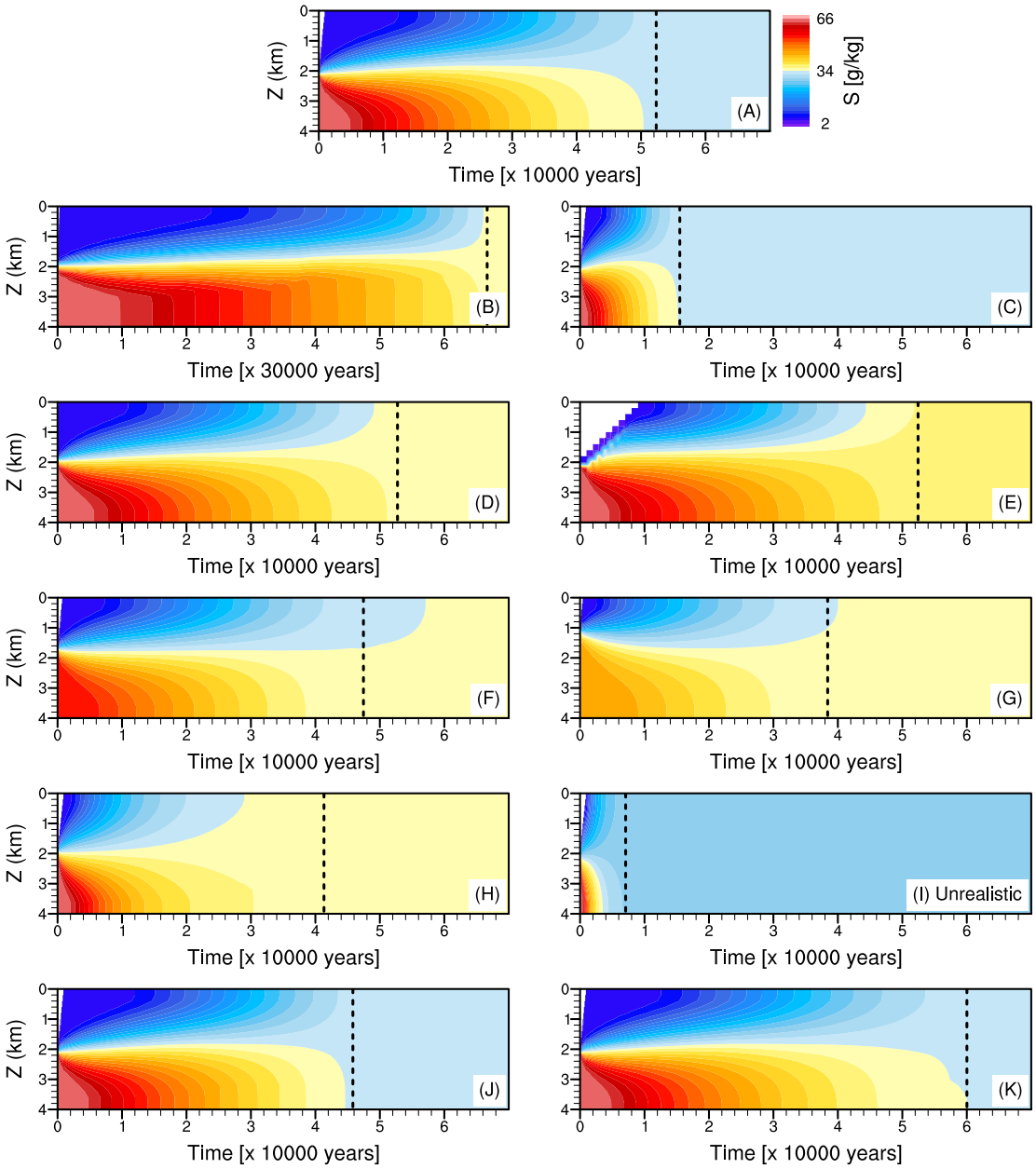

157

158 **Figure DR2: Evolution of ocean salinity of a post-snowball Earth under different**
159 **parameters. (A) The control experiment, same as Figure 2(A) in the main text for**
160 **comparison. (B) The mixing energy is 0.04 TW (versus 0.30 TW be default). (C) Same as B,**
161 **but for 1.10 TW. (D) The timescale of the freshwater entering the ocean is 100 years (versus**
162 **1000 years by default). (E) Same as D, but for 10,000 years. (F) The freshwater ocean depth**

is 1600 m (versus 2000 m by default). (G) Same as F, but for 1000 m. (H) The mixing coefficient is fixed to 6 x 10^{-6} m^2 s^{-1}. (I) Same as H, but for 3 x 10^{-5} m^2 s^{-1} (the modern Earth's mean value, but unrealistic for the post-snowball Earth). (J) The geothermal heat flux is 0.2 W m^{-2} (versus 0.1 W m^{-2} by default). (K) The geothermal heat flux is zero. The vertical dotted line denotes the time at which salinity becomes nearly uniform in depth (i.e., the difference of salinity between the sea surface and the ocean bottom is less than 1.0 g/kg). Note that the time interval in x-axis is 10,000 years in all of the panels except in (B) it is 30,000 years.